Case report

Elemental analysis of occupational granulomatous lung disease by electron probe microanalyzer with wavelength dispersive spectrometer: Two case reports

Hiromi Tomioka [a, *], Toshihiko Kaneda [a], Eiji Katsuyama [b], Masanori Kitaichi [c], Hiroshi Moriyama [d], Eiichi Suzuki [e]

[a] Department of Respiratory Medicine, Kobe City Medical Center West Hospital, 4, 2-chome, Ichibancho, Nagata-ku, Kobe 653-0013, Japan
[b] Department of Pathology, Kobe City Medical Center West Hospital, 4, 2-chome, Ichibancho, Nagata-ku, Kobe 653-0013, Japan
[c] Department of Pathology, National Hospital Organization, Kinki-Chuo Chest Medical Center, 1180 Nagasone-Cho, Kita-Ku, Sakai City, Osaka 591-8555, Japan
[d] Division of Respiratory Medicine, Graduate School of Medical and Dental Sciences, Niigata University, 1-757 Asahimachi-dori, Niigata 951-8510, Japan
[e] Department of General Medicine, Niigata University Medical and Dental Hospital, 1-757 Asahimachi-dori, Niigata 951-8510, Japan

A R T I C L E   I N F O

A B S T R A C T

The parenchymal lung diseases caused by metal inhalation include interstitial fibrosis, giant cell interstitial pneumonitis, chemical pneumonitis, and granulomatous disease, among others. We reported two cases of granulomatous lung disease with occupational exposure to metal dusts other than beryllium. They had worked in the battery manufacturing industry for 7 years and in an aluminum-processing factory for 6 years, respectively. Chest high-resolution computed tomography showed diffuse micronodules, and histology of video-assisted lung biopsy specimens revealed granulomatous lesions in the pulmonary interstitium. Results of microscopic examination of the tissue with special stains for mycobacteria and fungi were negative. Analysis by an electron probe microanalyzer with a wavelength-dispersive spectrometer (EPMA-WDS) confirmed the presence of silicon, iron, aluminum, and titanium in the granulomas. In particular, aluminum was distributed in a relatively high concentration in the granulomatous lesions. Although chronic beryllium disease is well known as an occupational granulomatous lung disease, much less is known about the other metals that cause granulomatous reactions in humans. Our report pointed out manifestations similar to beryllium disease after other metal dust exposures, in particular aluminum exposure. To our knowledge, this is the first report showing two-dimensional images of elemental mapping in granulomatous lesions associated with metal inhalation using EPMA-WDS.

1. Introduction

Various metal dusts and fumes can induce a wide range of lung pathology, including not only parenchymal diseases but airway disorders and cancer as well [1]. The parenchymal lung diseases caused by metal inhalation include interstitial fibrosis, giant cell interstitial pneumonitis, chemical pneumonitis, and granulomatous disease, among others [1]. Most of the disorders arise from occupational exposures. A granulomatous disease caused by beryllium, known as chronic beryllium disease since its description by Hardy and Tabershaw [2], is a representative occupational granulomatous lung disease. Similar manifestations are occasionally reported from other metal dust exposures, such as to aluminum, zirconium, titanium, earth metals, and talc, the latter of which contains various amounts of aluminum and silica [3–11]. However, reports have been limited that describe the clinical, radiographic, and pathological findings of conditions other than the

beryllium-induced granulomatous lung diseases as well as detailed information on mineralogical analyses of metal dusts.

An electron probe microanalyzer (EPMA) is an analytical tool used to non-destructively determine the chemical composition of small volumes of solid materials [12]. It irradiates specimens with a finely focused electron beam to obtain information about the elemental composition. Furthermore, EPMA with a wavelength-dispersive spectrometer (WDS) has higher sensitivity [13]. EPMA-WDS enables analysis of human lung tissue for deposits of elements by both qualitative and semi-quantitative methods [12]. We applied EPMA-WDS to biopsied lung tissue from patients presenting with granulomatous lung diseases with occupational exposure to metals other than beryllium to analyze the distribution of elements.

2. Case reports

2.1. Case 1

A 33-year-old man with a 12 pack-year history of cigarette smoking was referred to our hospital in 2006 because of exertional dyspnea. He had worked in the battery manufacturing industry for 7 years where he was exposed to cobalt, nickel, zinc, aluminum, and titanium. Beryllium was not used. He had begun working in that industry in 1998, and shortly thereafter developed skin eruptions with itching. In 2003, he was assigned by the company to a workplace dealing with cobalt hydroxide powder. There he developed an intense cough that was relieved after he left that workplace. He became aware of the onset of exertional dyspnea in 2004, and abnormal shadows on chest X-ray were detected at a health examination the next year. He left the industry and underwent examinations at a local hospital without a definite diagnosis. His past medical history included acute enteritis at the age of 30 years and depression at the age of 32 years. The patient's family history was unremarkable.

Physical examination revealed a well-developed, well-nourished man. On chest auscultation, fine crackles were heard subtly in both sides of the back and an abdominal examination revealed a smooth, non-tender liver edge 1 cm below the right costal margin.

No evidence of uveitis, cervical or supraclavicular lymphadenopathy, arthralgia, skin eruptions, or muscle weakness was found.

Laboratory investigations showed the following values: WBC count 5900/mm^3 with 2.5% eosinophils, Hb 15.8 g/L, C-reactive protein 0.7 mg/dL, aspartate aminotransferase 74 U/L, alanine aminotransferase 101 U/L, lactate dehydrogenase 254 IU/L, Υ-glutamyl transferase 417 U/L, creatinine 0.86 mg/dL, angiotensin converting enzyme (ACE) 24.0 U/L (normal range 6–21 U/L), serum KL-6 520 U/mL (normal range <500 U/mL), and surfactant protein D (SP-D) 30.5 ng/mL (normal range <110 ng/mL). Results of immunological tests were negative for autoimmune antibodies. Purified protein derivative (PPD) skin testing was positive at indurations of 15 mm × 15 mm. Arterial blood gas analysis while breathing room air revealed hypoxemia (PaO$_2$ 60.2 Torr), with PaCO$_2$ 38.3 Torr and pH 7.432. Although vital capacity (VC) was within normal range at 3.69 L (89.1%), both total lung capacity and carbon monoxide diffusing capacity (DLco) were reduced to 4.33 L (69.4%) and 12.09 mL/min/Torr (40.8%), respectively.

Chest X-ray showed faint infiltrative shadows in the bilateral outside lung fields (Fig. 1A). Chest high-resolution CT (HRCT) revealed micronodules, most prominent in the upper and middle lung zones with mediastinal lymph node enlargement (Fig. 1B). Bronchoalveolar lavage (BAL) fluids obtained previously at another hospital had 8.4 × 10^5 cells per mL and 3.6% neutrophils, 0.8% eosinophils, and 21.4% lymphocytes. The ratio of CD4 to CD8 T lymphocytes was 0.38.

A video-assisted lung biopsy was performed and histological findings of tissue obtained from the left S^{1+2} region are shown in Fig. 2. Numerous epithelioid cell granulomas predominantly in the pulmonary interstitium and hyalinous elastolytic fibrosis predominantly in the bronchiolovascular sheath were observed. Epithelioid cell granulomas were also observed in visceral pleura (not shown). No giant cell interstitial pneumonia pattern was found. Results of microscopic examination of the tissue with special stains for mycobacteria and fungi were negative.

Because he had an occupational exposure to several kinds of metals, examination of tissue sections with an EPMA-WDS was performed according to procedures previously described [12,14]. Briefly, with this procedure lung tissues are inflated, fixed with

(A)   (B)
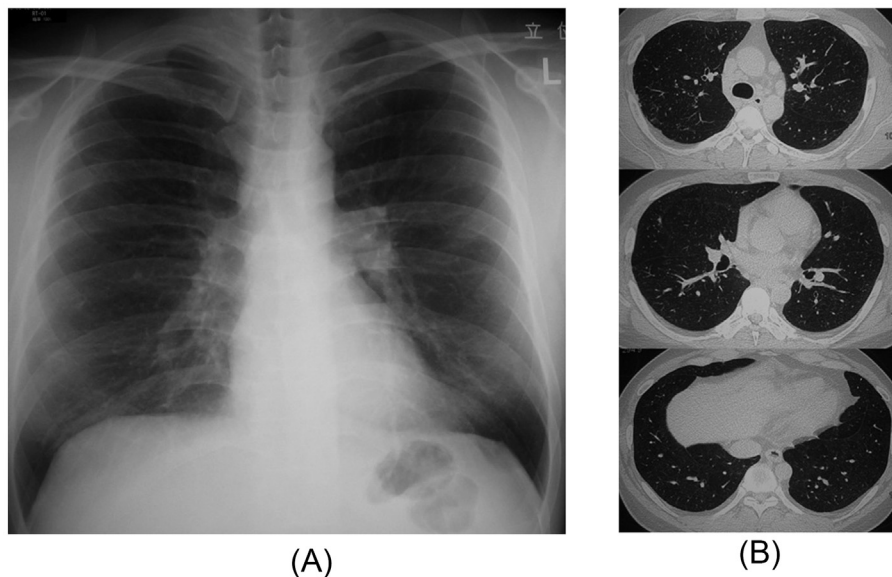
Fig. 1. Chest radiologic findings in Case 1. (A) Chest X-ray showed faint nodular shadows in the bilateral lung fields. (B) Chest high-resolution computed tomography shows diffuse fine nodular opacities that were distributed mainly in the upper and middle lung zones with mediastinal lymph node enlargement.

formalin, and then embedded in pure paraffin. 3- μm sections are floated on water drops on carbon blocks. Paraffin is thoroughly removed by xylene, and the sample is coated with carbon evaporation films. Serial thin sections of the sample are attached to an ultrapure carbon plate, then are dewaxed and processed for EPMA (EPMA 8705; Shimadzu Ltd., Kyoto, Japan)-WDS analysis and pathological examinations. EPMA images of a lung specimen are shown in Fig. 3, and results by quantitative analysis are shown in Table 1. Various metals mainly composed of silicon, iron, aluminum, and titanium were detected in a hyalinized granulomatous lesion (Table 1 Site 1). In particular, aluminum was widely distributed in the granulomatous lesion (Fig. 3B). Various elements including cobalt were also detected in the subpleural fibrotic lesion with black particle deposition (Table 1 Site 2). Tungsten was not detected.

As the patient had a mental disorder, after removal from the exposure he was followed up without corticosteroid therapy. Pulmonary function tests obtained 4 years after he left his job (in 2009) showed that VC and DLco were 3.58 L (76.6%) and 18.94 mL/min/Torr (63.6%), respectively. Final laboratory investigations obtained in 2010 showed the following values: ACE 28.5 U/L, serum KL-6 980 U/mL, and SP-D 33.0 ng/mL. Chest HRCT findings were not changed. No extrathoracic involvement that would indicate suspicion of sarcoidosis appeared.

2.2. Case 2

A 46-year-old man with no history of smoking was referred to our hospital in 2008 because of abnormal opacities on chest radiographs that were obtained at a local clinic where he had been treated for bronchial asthma. He had worked in an aluminum-processing factory for the past 6 years, from 1996 through 2001, where he had been exposed to aluminum dust. Beryllium was not used. He had not worn a protective mask. He had no signs of cough, dyspnea, fever, skin involvement, or arthritis. His past medical history included tuberculosis in childhood, gallstones at 21 years of age, and bronchial asthma at 43 years of age. His medications included theophylline, montelukast, olopatadine, beclometasone dipropionate, and fenoterol hydrobromide. With regard to family history, his mother had had tuberculosis.

Physical examination revealed a well-developed, well-nourished man. Chest auscultation revealed no abnormal findings, and there was no evidence of uveitis, cervical or supraclavicular lymphadenopathy, arthralgia, skin eruption, or muscle weakness.

Laboratory investigations showed the following values: WBC count 6280/mm^3 with 0.6% eosinophils, Hb 16.8 g/L, C-reactive protein 0.1 mg/dL, aspartate aminotransferase 17 U/L, alanine aminotransferase 17 U/L, lactate dehydrogenase 195 IU/L, ϒ-glutamyl transferase 21 U/L, creatinine 0.60 mg/dL, ACE 15.3 U/L, serum KL-6 291 U/mL, and SP-D 25.0 ng/mL. QuantiFERON TB-2G testing (Cellestis, Carnegie, Australia) was positive with culture filtrate protein-10 of 5.14 IU/mL, and the 6-kDa early secretory antigenic target of Mycobacterium tuberculosis was 0.20 IU/mL (normal range <0.35 IU/mL). PPD skin testing was positive for indurations of 27 mm × 24 mm. Arterial blood gas analysis while breathing room air did not reveal hypoxemia (PaO$_2$ 90.3 Torr), with PaCO$_2$ 39.7 Torr and pH 7.433. Pulmonary function tests showed the following values: VC 3.05 L (83.7%) and forced expiratory volume in 1 s 2.53 L (78.6%). Diffuse nodular shadows were found on chest X-ray (Fig. 4A), and chest HRCT showed diffuse nodular opacities with interlobular septal thickening (Fig. 4B). In BAL fluids there were 3.1 × 10^5 cells per mL, with 1.0% neutrophils, 18.5% lymphocytes, and 80.5% macrophages. The ratio of CD4 to CD8 T lymphocytes was 0.94. BAL fluid cultures and acid-fast bacillus PCR were free of pathogens. Histology performed on transbronchial biopsies did not

reveal granuloma and no definite diagnosis could be made. Anti-tuberculosis drug therapy using rifampicin, isoniazid, ethambutol, and pyrazinamide for 3 months did not improve the chest HRCT findings. Then a video-assisted lung biopsy was performed. Results of histology of tissue obtained from the right S^3 region are shown in Fig 5. Granulomatous lesions mainly composed of multinucleated giant cells were observed predominantly in the pulmonary interstitium. Results of microscopic examination of the tissue with special stains for mycobacteria and fungi were negative. Hemosiderosis and anthracosis with pneumoconiotic materials were also observed (not shown). Elemental analysis was performed for the granuloma (Fig. 6A) and the centrilobular fibrosing lesion (Fig. 6C). Silicon, aluminum, iron, and titanium were detected in both lesions (Table 1 Site 3 and 4). Especially wide distribution of aluminum was observed in the granuloma (Fig. 6B).

The patient was followed up without special medication though 2014 when his chest HRCT findings showed no changes and he was without respiratory symptoms.
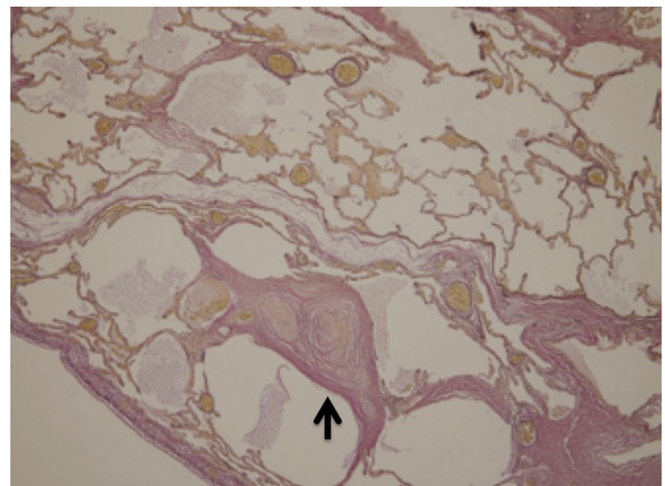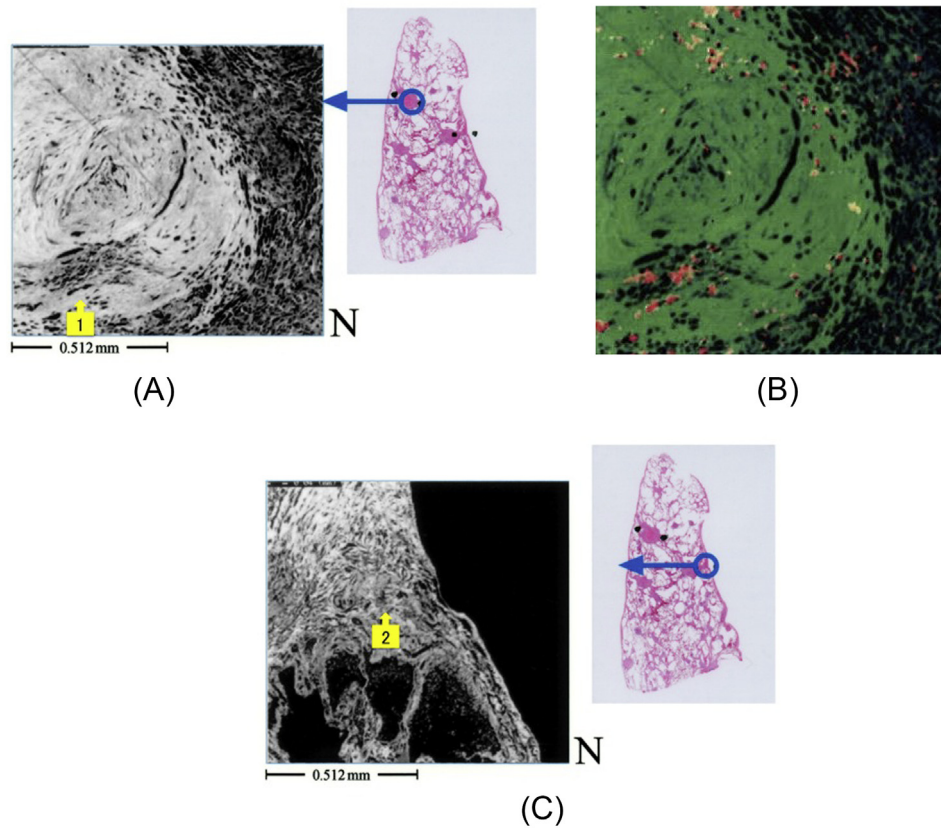

(A)
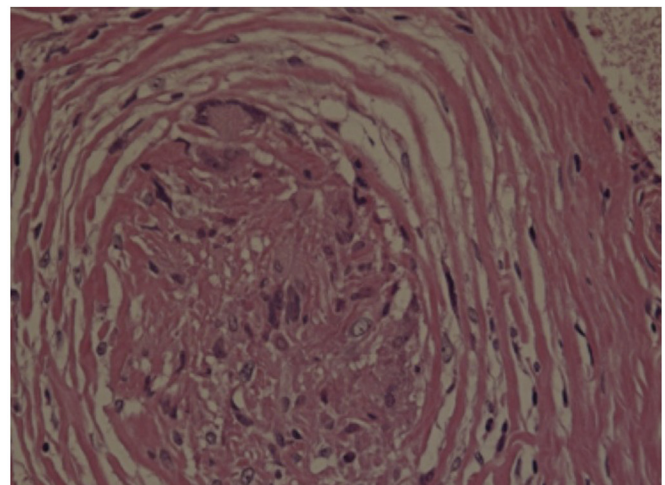
(B)

Fig. 2. Histological findings from surgical lung biopsy specimen from the left S^{1+2} region in Case 1 (A,B). Epithelioid cell granuloma (arrow) in the pulmonary interstitium and hyalinous elastolytic fibrosis predominantly in the bronchiolovascular sheath (hematoxylin and eosin stain, 20 × and 40 ×).

Fig. 3. Electron probe microanalyzer images of a lung specimen from Case 1. (A) Gray scale image (left) of the granulomatous lesion obtained from the circled region in the lung specimen stained with hematoxylin and eosin (right). A square, 10 × 10 μm, indicated by the yellow arrowhead numbered 1, was quantitatively analyzed, with results shown in Table 1 Site 1. (B) Qualitative color image of aluminum distribution is superimposed on the lung tissue image with amino nitrogen colored green. Because the distribution of amino nitrogen corresponds to the pathologic image, detected elements colored red are easily localized in the lung specimen. (C) Gray scale image (left) of the subpleural lesion with black particle deposition obtained from the circled region in the lung specimen stained with hematoxylin and eosin (right). A square, 10 × 10 μm, indicated by the yellow arrowhead numbered 2, was quantitatively analyzed, with results shown in Table 1 Site 2.

3. Discussion

We reported here two cases of granulomatous lung disease with occupational exposure to metals. The first case had worked in the battery manufacturing industry for 7 years and the second case had worked in an aluminum-processing factory for 6 years. Both men were exposed to metals other than beryllium, and analysis by EPMA-WDS confirmed the presence of silicon, iron, aluminum, and titanium in the granulomas. Although chronic beryllium disease is well known as an occupational granulomatous lung disease, much less is known about the other metals that cause granulomatous reactions in humans. Silicon, aluminum, and iron are commonly found in healthy human lung, however, wide distribution of aluminum was observed in the granulomatous lesions in both cases. Our report pointed out manifestations similar to beryllium disease after other metal dust exposures, in particular aluminum exposure.

A number of pulmonary effects have been attributed to aluminum exposure including bronchial asthma, chronic bronchitis, pulmonary fibrosis, granulomatous lung disease, acute tracheobronchitis, pneumonitis, alveolar proteinosis, and pulmonary edema [1,11]. Pneumoconiosis caused by the presence of dust containing aluminum in lung tissue is known as pulmonary aluminosis. It is caused by the exposure to aluminum and its compounds under diverse occupational circumstances and factors [15]. Of these granulomatous lung diseases, those induced by aluminum

Table 1
Electron probe microanalyzer results by quantitative analysis.

Case 1				Case 2			
Site 1		Site 2		Site 3		Site 4	
O	54.954%	O	37.343%	Si	36.373%	Fe	68.914%
Si	26.768%	Si	20.404%	O	29.720%	O	14.449%
Al	13.790%	Fe	12.546%	Fe	15.203%	Si	5.957%
K	2.132%	Al	11.264%	Al	8.927%	P	2.469%
Fe	0.558%	Ti	7.497%	K	2.778%	Al	2.381%
S	0.328%	K	6.019%	Ca	1.688%	Ca	2.307%
Ca	0.304%	Mg	1.696%	Ti	1.567%	S	0.970%
Ba	0.277%	Ca	0.840%	Mg	1.184%	Zn	0.823%
P	0.263%	P	0.638%	Na	1.071%	Ti	0.697%
Ti	0.248%	Zn	0.477%	P	0.780%	K	0.473%
Mg	0.246%	S	0.376%	S	0.709%	Mg	0.614%
Na	0.131%	Ni	0.253%			Na	0.196%
		Co	0.244%				
		Mn	0.203%				
		Na	0.120%				
		Cl	0.080%				

In Case 1 various metals, mainly silicon, iron, aluminum, and titanium, were detected in hyalinized granulomatous lesion (Site 1) and those including cobalt were detected in the subpleural fibrotic lesion (Site 2). In Case 2 various metals mainly composed of silicon, aluminum, iron, and titanium were detected in the granuloma (Site 3) and centrilobular fibrosing lesion (Site 4).

Fig. 4. Chest radiologic findings in Case 2. (A) Chest X-ray showed diffuse nodular shadows (B). Chest high-resolution computed tomography shows diffuse nodular opacities with interlobular septal thickening.

dust are rare. Chen et al. [4] reported the first case of pulmonary granulomatosis associated with aluminum-containing welding fumes. De Vuyst et al. [5] reported a case of sarcoid-like granulomatosis in a chemist who worked with aluminum powders. Lung granulomatosis attributed to occupational exposure to beryllium and aluminum was also reported in a dental laboratory technician [16]. Later Cai et al. [6] reported a case of sarcoid-like granulomatosis induced by aluminum dust in a metal reclamation factory worker. Based upon their occupational histories, in our cases after exclusion of infectious agents and the performance of combined histological and mineralogical studies, aluminum dust could account for the development of pulmonary granulomas.

The exact pathogenesis of aluminum-induced diseases of lung parenchyma is unknown [15]. Kraus et al. [17] conducted a cross-sectional study to detect early stages of aluminosis using HRCT in two plants that produced aluminum powder in Germany. They
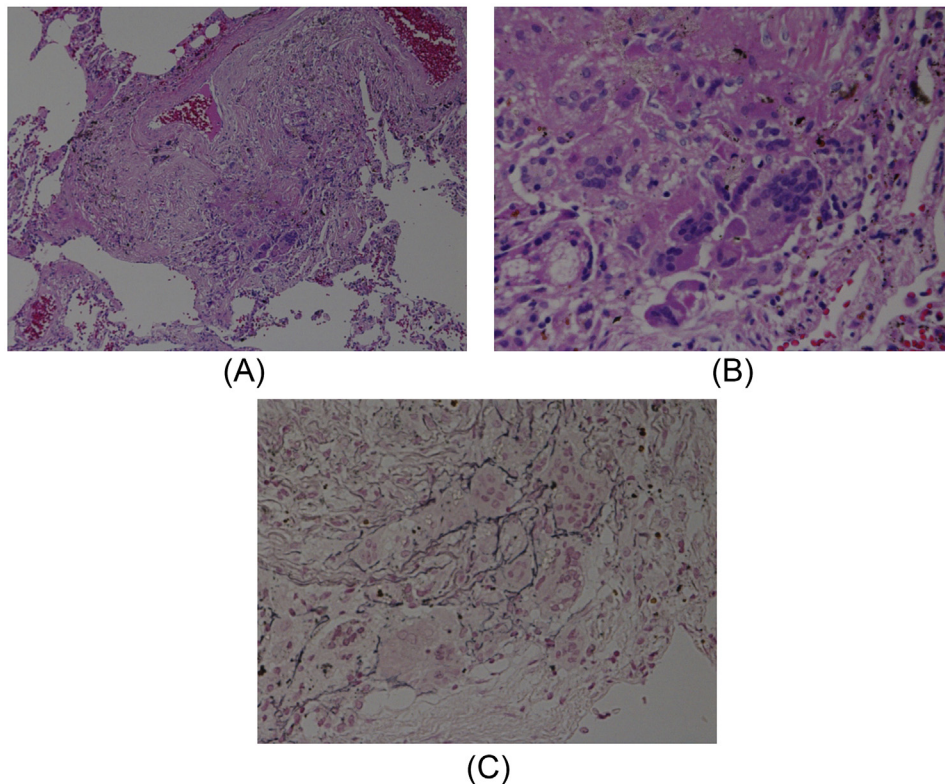
Fig. 5. Histological findings in surgical lung biopsy from the right S³ region in Case 2. (A,B) granulomatous lesion mainly composed of multinucleated giant cells in adventitia of pulmonary muscular artery (hematoxylin and eosin stain, 10 × and 40 ×); (C) argyrophilic fiber formation around multinucleated giant cells (silver stain, 40 ×).

found small rounded and ill-defined centrilobular opacities mainly in the upper lobes in 15 of 62 highly exposed workers. Their reported CT findings resembled those in our cases. Although no biopsy results were available in their study, some of their cases might have had granulomatous lung disease with occupational exposure to aluminum, as with our cases. That study also showed that not all highly exposed workers with plasma and urinary concentrations of aluminum were found to have parenchymal changes. Therefore, individual susceptibility is suggested to play an important role in the development of aluminosis [17].

In addition to exposure to aluminum, Case 1 was exposed to cobalt, nickel, zinc, and titanium. These metals were identified in the granulomatous lesion by elemental analysis using EPMA-WDS, although only very small amounts of titanium were found. Redline et al. [18] reported a case of granulomatous disease associated with pulmonary deposition of titanium. The patient had worked as a furnace feeder for an aluminum smelting company where he was exposed to various metallic fumes and dusts released in the production of aluminum and zinc alloys. Scanning electron microscopy with energy dispersive X-ray analysis of a transbronchial biopsy specimen from the patient's lung showed that the pulmonary granulomas contained large numbers of metallic particulates of aluminum with titanium and other metals. They suggested an etiological role between the inhalation of titanium and a granulomatous disease process based on cellular immunological studies that showed abnormal lymphocyte transformation tests to titanium chloride and normal responses to aluminum, nickel, and beryllium. We did not perform cellular immunological studies; however, titanium might also have been associated with the granulomatous lung disease in our Case 1.

Furthermore we must mention the association of cobalt in this case. Cobalt exposure alone has been rarely associated with parenchymal lung disease. This led to the widespread belief that simultaneous inhalation of other metals such as tungsten carbide is essential for development of parenchymal disease [19]. Hard metal is a synthetic compound that combines tungsten carbide with cobalt as well as a number of other metals, and some hard metal exposures have resulted in manifestations of granulomatous pneumonitis [20,21]. Case 1 was exposed to cobalt but did not use tungsten, so hard metal disease is not indicated. In fact, pathological findings in this case did not show the presence of bizarre, cannibalistic, giant, multinucleated cells, a hallmark of hard metal disease, classically seen in giant cell interstitial pneumonia [22]. However cobalt is never found in healthy subjects, so the element might be pathogenetic to Case 1.

Interestingly, an elevation in serum ACE levels was observed in Case 1, so the differential diagnosis in this case included sarcoidosis. However, the following findings indicate negativity for sarcoidosis: positive PPD skin test, BAL fluid findings without elevation of the ratio of CD4 to CD8 T lymphocytes, and no extrathoracic involvement including uveitis in the follow-up period. Serum levels of ACE are elevated in a variety of granulomatous disorders, including not only sarcoidosis [23,24] but also silicosis [24,25], miliary tuberculosis [24], berylliosis [26], and leprosy [27]. Smolková et al. [28] reported a case of occupational pulmonary aluminosis presenting with numerous dispersed micronodules and bilateral hilar enlargement on chest images in which sarcoidosis was first diagnosed without detailed knowledge of occupational history. The clinical and pathological similarities between metal-induced disease and sarcoidosis should be recognized [11].

Various techniques can be employed in the evaluation of mineral dusts within lung tissues. We applied EPMA-WDS to biopsied
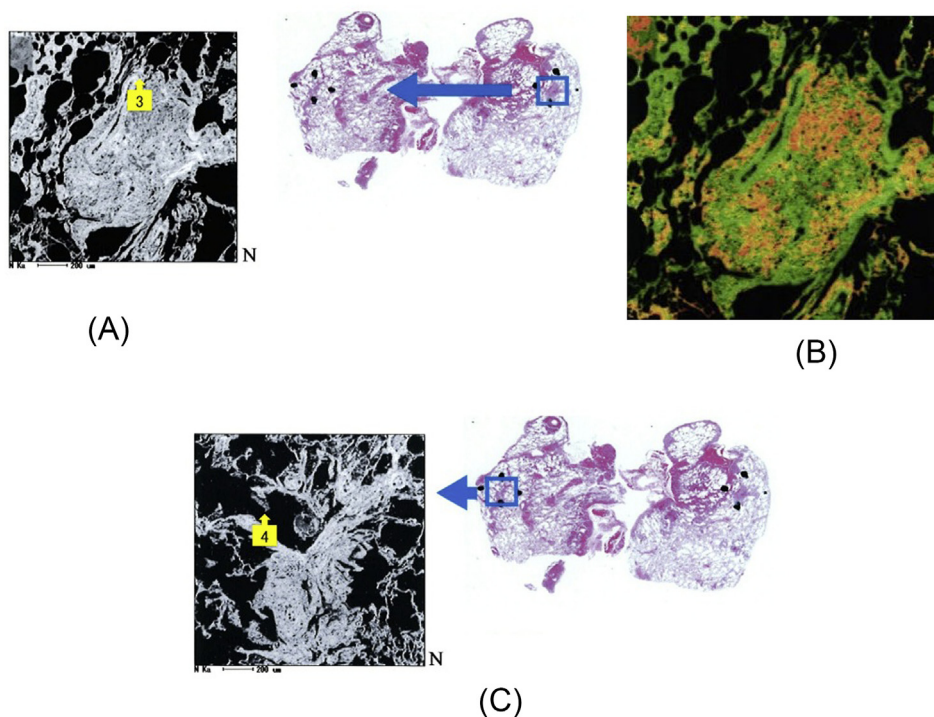
Fig. 6. Electron probe microanalyzer images of a lung specimen from Case 2. A) Gray scale image (left) of the granulomatous lesion obtained from the squared region in the lung specimen stained with hematoxylin and eosin (right). A square, 10 × 10 μm, indicated by the yellow arrowhead numbered 3, was quantitatively analyzed, with results shown in Table 1 Site 3. (B) Qualitative colored image of aluminum distribution (colored red) is superimposed on the lung tissue image with amino nitrogen colored green. (C) Gray scale image (left) of the fibrosing lesion around the bronchiole obtained from the squared region in the lung specimen stained with hematoxylin and eosin (right). A square, 10 × 10 μm, indicated by the yellow arrowhead numbered 4, was quantitatively analyzed, with results shown in Table 1 Site 4.

lung tissue from two patients with occupational granulomatous lung disease. This technique can produce elemental distribution maps that can be subsequently compared to the pathology of a serial tissue section [12]. Although most studies that have analyzed organic samples by EPMA used an energy dispersive spectrometer, WDS is almost 10 times more sensitive than energy dispersive spectrometer for all elements (13). EPMA-WDS is useful to analyze the distribution of elements in hard metal lung disease [29]. Therefore, the use of this technique provided an accurate identification of the deposits observed within the granulomatous lesions and supported a causal association with the type of exposure reported by the patient and his granulomatous lung disease. To our knowledge, this is the first report showing two-dimensional images of elemental mapping in granulomatous lesions associated with metal inhalation using this method.

In summary, metal dusts other than beryllium can induce granulomatous lung diseases. EPMA-WDS is a promising technique for mineralogical analysis of lung samples from patients with occupational granulomatous lung diseases.

Acknowledgements

References

[1] P. Kelleher, K. Pacheco, L.S. Newman, Inorganic dust pneumonias: the metal-related parenchymal disorders, Environ. Health Perspect. 108 (Suppl. 4) (2000) 685–696.

[2] H.L. Hardy, I.R. Tabershaw, Delayed chemical pneumonitis in workers exposed to beryllium compounds, J. Ind. Hyg. Toxicol. 28 (1946) 197–211.

[3] M. Drent, P.H. Bomans, R.J. Van Suylen, R.J. Lamers, A. Bast, E.F. Wouters, Association of man-made mineral fibre exposure and sarcoidlike granuloma, Respir. Med. 94 (8) (2000) 815–820.

[4] W.J. Chen, R.J. Monnat Jr., M. Chen, N.K. Mottet, Aluminum induced pulmonary granulomatosis, Hum. Pathol. 9 (6) (1978) 705–711.

[5] P. De Vuyst, P. Dumortier, L. Schandene, M. Estenne, A. Verhest, J. Yernault, Sarcoidlike lung granulomatosis induced by aluminum dusts, Am. Rev. Respir. Dis. 135 (2) (1987) 493–497.

[6] H.R. Cai, M. Cao, F.Q. Meng, J.Y. Wei, Pulmonary sarcoid-like granulomatosis induced by aluminum dust: report of a case and literature review, Chin. Med. J. 120 (17) (2007) 1556–1560.

[7] C. Voisin, F. Fisekci, B. Buclez, et al., Mineralogical analysis of the respiratory tract in aluminium oxide-exposed workers, Eur. Respir. J. 9 (9) (1996) 1874–1879.

[8] R. Orriols, J. Ferrer, J.M. Tura, C. Xaus, R. Coloma, Sicca syndrome and silicoproteinosis in a dental technician, Eur. Respir. J. 10 (3) (1997) 731–734.

[9] T.L. Schauble, E.A. Rich, Lymphocytic alveolitis in a crematorium worker, Chest 105 (2) (1994) 617–619.

[10] C. Gysbrechts, E. Michiels, E. Verbeken, et al., Interstitial lung disease more than 40 years after a 5 year occupational exposure to talc, Eur. Respir. J. 11 (6) (1998) 1412–1415.

[11] L.S. Newman, Metals that cause sarcoidosis, Semin. Respir. Infect. 13 (3) (1998) 212–220.

[12] T. Takada, H. Moriyama, E. Suzuki, Elemental analysis of occupational and environmental lung diseases by electron probe microanalyzer with wavelength dispersive spectrometer, Respir. Investig. 52 (1) (2014) 5–13.

[13] J.I. Goldstein, D.E. Newbury, P. Echlin, et al., Scanning Electron Microscopy and X-ray Microanalysis, Plenum Press, New York, 1994, pp. 499–501.

[14] K. Watanabe, O. Miyakawa, M. Kobayashi, New method for quantitative mapping of metallic elements in tissue sections by electron probe microanalyser with wavelength dispersive spectrometers, J. Electron Microsc. (Tokyo) 50 (1) (2001) 77–82.

[15] P. Smolkova, M. Nakladalova, The etiology of occupational pulmonary aluminosis-the past and the present, Biomed. Pap. Med. Fac. Univ. Palacky. Olomouc Czech Repub. 158 (4) (2014) 535–538.

[16] P. Brancaleone, B. Weynand, P. De Vuyst, D. Stanescu, T. Pieters, Lung granulomatosis in a dental technician, Am. J. Ind. Med. 34 (6) (1998) 628–631.

[17] T. Kraus, K.H. Schaller, J. Angerer, R.D. Hilgers, S. Letzel, Aluminosis- detection of an almost forgotten disease with HRCT, J. Occup. Med. Toxicol. 1 (2006) 4.

[18] S. Redline, B.P. Barna, J.F. Tomashefski Jr., J.L. Abraham, Granulomatous disease associated with pulmonary deposition of titanium, Br. J. Ind. Med. 43 (10) (1986) 652–656.

[19] B. Swennen, J.P. Buchet, D. Stanescu, D. Lison, R. Lauwerys, Epidemiological survey of workers exposed to cobalt oxides, cobalt salts, and cobalt metal, Br. J. Ind Med. 50 (9) (1993) 835–842.

[20] E.O. Coates Jr., J.H. Watson, Diffuse interstitial lung disease in tungsten carbide workers, Ann. Intern Med. 75 (5) (1971) 709–716.

[21] A. Satoh-Kamachi, M. Munakata, Y. Kusaka, et al., A case of sarcoidosis that developed three years after the onset of hard metal asthma, Am. J. Ind. Med. 33 (4) (1998) 379–383.

[22] S. Anttila, S. Sutinen, M. Paananen, et al., Hard metal lung disease: a clinical, histological, ultrastructural and X-ray microanalytical study, Eur. J. Respir. Dis. 69 (2) (1986) 83–94.

[23] G.M. Ainslie, S.R. Benatar, Serum angiotensin converting enzyme in sarcoidosis: sensitivity and specificity in diagnosis: correlations with disease activity, duration, extra-thoracic involvement, radiographic type and therapy, Quart. J. Med. 55 (218) (1985) 253–270.

[24] E.A. Brice, W. Friedlander, E.D. Bateman, R.E. Kirsch, Serum angiotensin-converting enzyme activity, concentration, and specific activity in granulomatous interstitial lung disease, tuberculosis, and COPD, Chest 107 (3) (1995) 706–710.

[25] C. Grönhagen-Riska, K. Kurppa, F. Fyhrquist, O. Selroos, Angiotensin- converting enzyme and lysozyme in silicosis and asbestosis, Scand. J. Respir. Dis. 59 (4) (1978) 228–231.

[26] L.A. Maier, M.V. Raynolds, D.A. Young, E.A. Barker, L.S. Newman, Angiotensin-1 converting enzyme polymorphisms in chronic beryllium disease, Am. J. Respir. Crit. Care Med. 159 (4 Pt 1) (1999) 1342–1350.

[27] J. Lieberman, T.H. Rea, Serum angiotensin-converting enzyme in leprosy and coccidioidomycosis, Ann. Intern Med. 87 (4) (1977) 423–425.

[28] P. Smolková, M. Nakládalová, T. Tichý, M. Hampalová, V. Kolek, Occupational pulmonary aluminosis: a case report, Ind. Health 52 (2) (2014) 147–151.

[29] H. Moriyama, M. Kobayashi, T. Takada, et al., Two-dimensional analysis of elements and mononuclear cells in hard metal lung disease, Am. J. Respir. Crit. Care Med. 176 (1) (2007) 70–77.